



## Article

# Low-Cost Sensor for Lycopene Content Measurement in Tomato Based on Raspberry Pi 4

Marcos-Jesús Villaseñor-Aguilar <sup>1,2</sup>, José-Alfredo Padilla-Medina <sup>2</sup>, Juan Prado-Olivarez <sup>2</sup>,  
José-Errique Botello-Álvarez <sup>2</sup>, Micael-Gerardo Bravo-Sánchez <sup>2</sup> and Alejandro-Israel Barranco-Gutiérrez <sup>2,\*</sup>

<sup>1</sup> Departamento de Ingeniería de Robótica y de Datos, Universidad Politécnica de Guanajuato, Cortazar 38496, Mexico; mvillaseñor@upgto.edu.mx

<sup>2</sup> Tecnológico Nacional de México en Celaya, Celaya 38010, Mexico; alfredo.padilla@itcelaya.edu.mx (J.-A.P.-M.); juan.prado@itcelaya.edu.mx (J.P.-O.); enrique.botello@itcelaya.edu.mx (J.-E.B.-Á.); gerardo.bravo@itcelaya.edu.mx (M.-G.B.-S.)

\* Correspondence: israel.barranco@itcelaya.edu.mx

**Abstract:** Measuring lycopene in tomatoes is fundamental to the agrifood industry because of its health benefits. It is one of the leading quality criteria for consuming this fruit. Traditionally, the amount determination of this carotenoid is performed using the high-performance liquid chromatography (HPLC) technique. This is a very reliable and accurate method, but it has several disadvantages, such as long analysis time, high cost, and destruction of the sample. In this sense, this work proposes a low-cost sensor that correlates the lycopene content in tomato with the color present in its epicarp. A Raspberry Pi 4 programmed with Python language was used to develop the lycopene prediction model. Various regression models were evaluated using neural networks, fuzzy logic, and linear regression. The best model was the fuzzy nonlinear regression as the RGB input, with a correlation of  $R^2 = 0.99$  and a mean error of  $1.9 \times 10^{-5}$ . This work was able to demonstrate that it is possible to determine the lycopene content using a digital camera and a low-cost integrated system in a non-invasive way.



**Citation:** Villaseñor-Aguilar, M.-J.; Padilla-Medina, J.-A.; Prado-Olivarez, J.; Botello-Álvarez, J.-E.; Bravo-Sánchez, M.-G.; Barranco-Gutiérrez, A.-I. Low-Cost Sensor for Lycopene Content Measurement in Tomato Based on Raspberry Pi 4. *Plants* **2023**, *12*, 2683. <https://doi.org/10.3390/plants12142683>

Academic Editors: Ivo Vaz de Oliveira and Sílvia Martins Afonso

Received: 18 May 2023

Revised: 17 June 2023

Accepted: 28 June 2023

Published: 18 July 2023



**Copyright:** © 2023 by the authors. Licensee MDPI, Basel, Switzerland. This article is an open access article distributed under the terms and conditions of the Creative Commons Attribution (CC BY) license (<https://creativecommons.org/licenses/by/4.0/>).

**Keywords:** artificial neuronal network; fuzzy logic; HPLC; image; lycopene; Raspberry Pi 4; tomato

## 1. Introduction

Fresh tomatoes are the most consumed fruit worldwide for their nutritional value and health benefits [1]. In 2021, the United Nations Food and Agriculture Organization (FAO) reported that world tomato production was more than 189 million tons [2]. It should be noted that tomatoes are a nutritional source of potassium, vitamin E, A, C, phosphorus, and antioxidants. The intake of this vegetable prevents the development of lung, stomach, and prostate cancer and cardiovascular diseases [3].

Traditionally, the harvest moment of this fruit is terminated visually by a farmer, who identifies the different degrees of maturity [4]. Nevertheless, this process can be affected by lighting, environmental conditions, and a lack of harvester experience [5]. The tomato ripening process involves physiological and biochemical changes that include ethylene, carotenoids, and cell wall metabolism [6,7]. Lycopene is a linear carotenoid that synthesizes through a pathway starting from geranyl diphosphate [8]. It accounts for about 80–90% of the carotenoids found in tomatoes. This is a natural pigment that generates the red coloration, which is used as a quality parameter by consumers [9,10]. Furthermore, lycopene has a high economic impact on the development of products in the pharmaceutical industry, such as clinical products, shakes, vitamins, proteins, and sports supplements [11].

The conventional technique used in laboratories for the measurement of lycopene is high-performance liquid chromatography (HPLC). This is a technique for separating non-volatile or thermolabile species from a sample using chemical interactions between

the analyte and the chromatographic column [12]. Measurements made with HPLC are represented by a chromatogram. The measurement process using HPLC is costly in terms of time and money. In addition, another drawback of HPLC is the invasion of the fruit to obtain a homogeneous sample that will facilitate the extraction process of the lycopene. This is performed with the use of highly toxic chemical solvents such as ethanol, acetone, petroleum ether, hexane, benzene, chloroform itself, or their combinations [13,14].

On the other hand, color measurement is one of the unconventional laboratory techniques that correlates with lycopene. The CIEL\*a\*b\* color space model is the most widely used due to its ability to classify the stages of tomato maturity. This is used because the \*a axis is sensitive to changes in color from red to green and, in the case of the \*b axis, from yellow to blue. This carotenoid can be estimated using the color descriptors \*a, \*a/\*b, (\*a/\*b)<sup>2</sup>, hue, and chroma. Regarding the ratio a\*/b\*, it is commonly used in the generation of mathematical models due to its low computational cost. It should be noted that the color measurement of the samples is carried out with laboratory equipment under controlled conditions, such as the Konica-Minolta CR200, CR400, CR410, and CM-2002. Another device used is the Ocean Optics STS-VIS detector, a spectrometer with a fiber optic input. This has been used to develop a portable LED-based colorimeter using the reflectance spectrum of tomato in the range of 400–750 nm, estimating lycopene concentrations of 70 and 550 mg × kg of fresh weight skin. Another widely used technique is Vis-NIR spectra; this technique presents slightly better results in predicting lycopene than using the ratio a\*/b\* [15–19].

It is necessary to highlight that the Raspberry-Pi-embedded system has become very important in scientific and engineering applications [20]. For example, it helps eliminate the subjectivity and complexity of the measurement systems of the physicochemical properties and quality parameters of fruits on a minicomputer design and camera [21–26]. The present work proposed a methodology for developing a non-invasive sensor for measuring tomato lycopene in situ. The sensor uses artificial vision and artificial intelligence techniques implemented on a Raspberry Pi 3. The device operates using various optical filters that improve the spectral selectivity of the images to be processed. Together, it has an innovative structure made by 3D printing that eliminates lighting variations.

This work is composed of four sections. Section 2 shows the results of the mathematical models based on artificial neuronal networks and fuzzy logic. Section 3 presents the results of the mathematical models based on artificial neuronal networks and fuzzy logic. Subsequently, Section 4 indicates the materials and methods used to design the sensor. This section considers how the samples were chosen, the analysis using HPLC, and the sensor configuration process. Section 5 presents the conclusions.

## 2. Results

Figures 1 and 2 show the measurements and errors of the models proposed in the sensor. The measurements made with the HPLC for each sample can be seen in Figure 1. These correspond to eighteen circular green markers. It can be seen that the best model was Model 4, which used the RGB components as input, with a correlation of 0.99 and an average error of  $1.9 \times 10^{-5}$ . Model 4 has a 99% coincidence with the measurements made by the HPLC. Models 5 and 6 presented slightly lower results with average errors of  $9.3973 \times 10^{-5}$  and  $-7.8450 \times 10^{-4}$ . For the case of Models 2 and 3, their correlation is more significant than 0.9. Model 1 presented difficulties in determining the content of maturity stages turning to red. This is reflected in the increase in its average error, as shown in Figure 2.

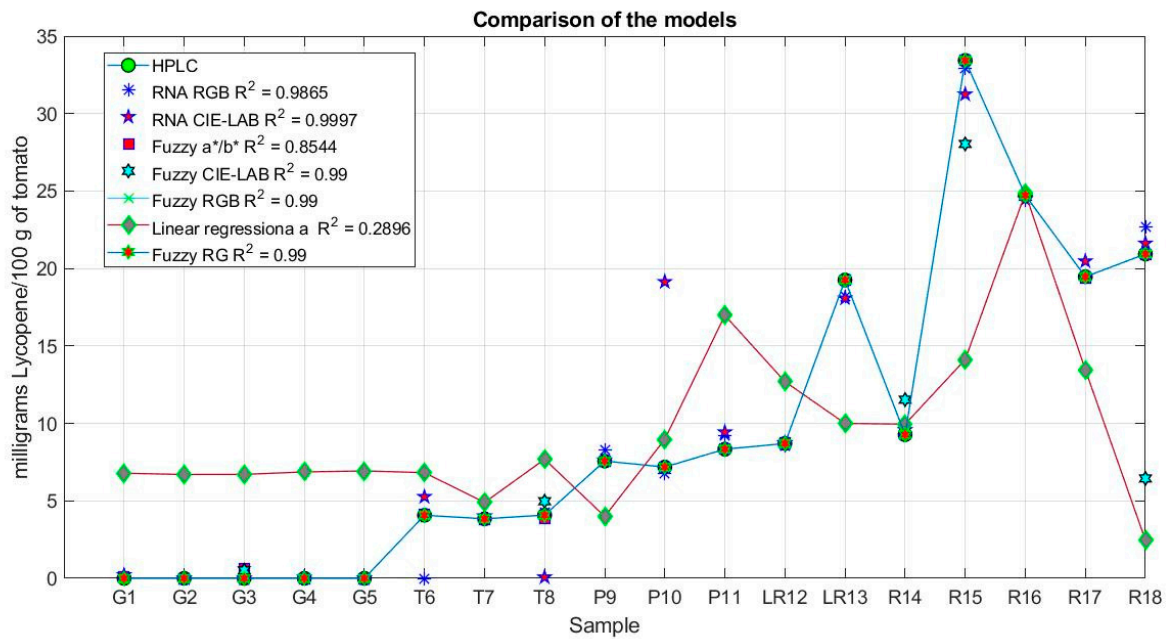


Figure 1. Predictions of the sensor models.

Figure 2 shows the average error for Model 3 and Model 6. They are very near to zero. Together, it can be seen that Model 6 presents the most significant error of 6.29%.

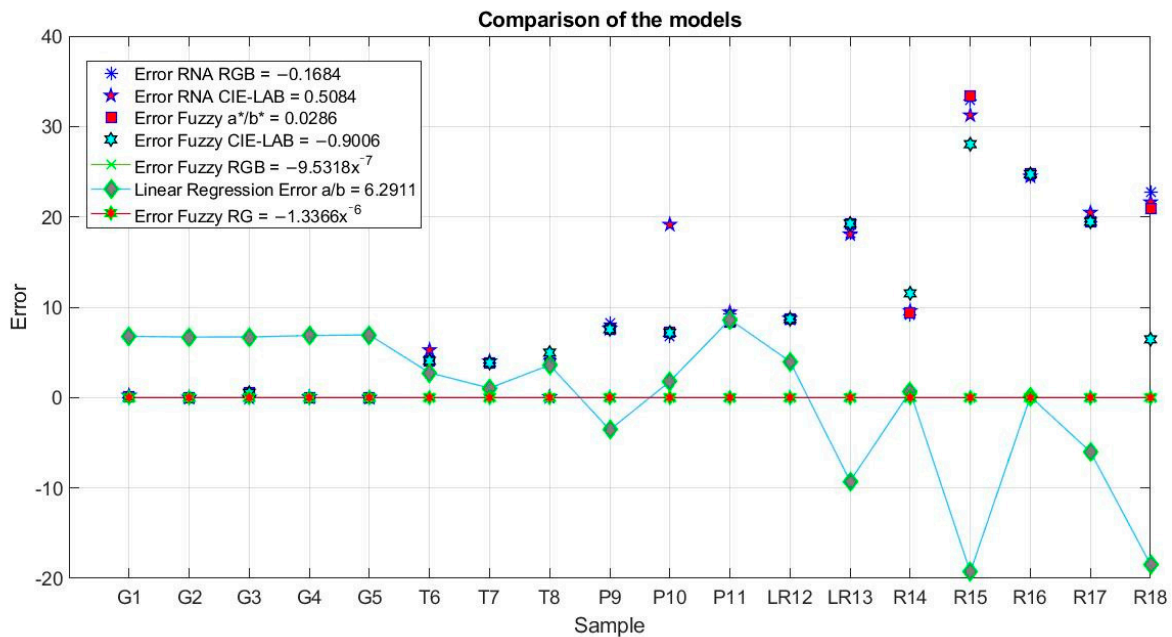
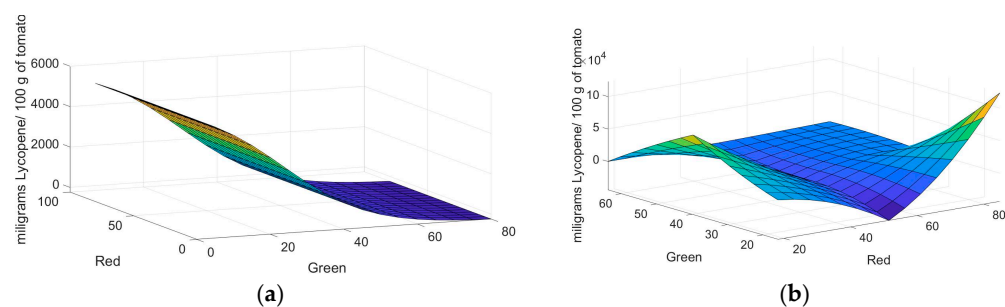


Figure 2. Average error of the predictions of sensor models.

In order, Figure 3 shows the response of the proposed Model 1 and Model 3. Both models can observe an increase in the lycopene content of the samples when the red pixels increase and the green pixels decrease. The increase in lycopene is related to the change in the tomato’s maturity. These results coincide with the visual classification of the samples by their degree of maturity and present a good correlation with the measurements made by the proposed sensor and the high-performance liquid chromatography (HPLC).



**Figure 3.** Resulting surface from the causality of the red and green inputs in the proposed models. (a) Model based on ANNs using sigmoidal-type activation functions. (b) Model based on FL using triangular-type membership functions.

### 3. Discussion

The main contribution of this work is the design, construction, and testing of a sensor to measure lycopene in tomatoes in the field without destroying them, calibrated with HPLC and with qualities such as portability, high reliability, low energy consumption, and low cost. Table 1 shows the comparison of the different models. To find the best estimate, several mathematical models were created; for example, Model 4 was the one that presented a good correlation of  $R^2 = 0.99$  and the lowest prediction error, which was  $1.9 \times 10^{-5}$ . Table 1 shows different proposals that include Models 5 and 6 that presented a high correlation with the lycopene content using the chromatic transformation  $*a/*b$ , as well as other proposals reported in the literature. These results coincide with what was reported by [15,18]. Together, the models that used multiple nonlinear regression show a higher correlation that is consistent with that reported by [27]. This sensor analyzes most of the surface of the epicarp of the fruit, which differs from that reported by [4,15], who performed a specific local analysis. Being non-destructive, this device allows it to be used as a tomato traceability tool from cultivation, harvest, transport, storage, and sale until consumption [28].

**Table 1.** Comparison of the different models.

Models	Technique	Input	$R^2$	Error Mean
Model 1	MNNR	R, G, B	0.98	0.1684
Model 2	MNNR	$L^*$ , $*a$ , $*b$	0.90	0.5084
Model 3	MNFR	R, G, B	0.99	$-9.53 \times 10^{-7}$
Model 4	MNFR	$L^*$ , $*a$ , $*b$	0.99	0.9006
Model 5	MNFR	$*a/*b$	0.99	0.0286
Model 6	MNFR	R, G	0.99	0.9006
(Arias et al., 2000) [15]	LR	$L^*$ , $*a$ , $*b$	0.90	6.2911
(Vazquez-Cruz et al., 2013) [17]	MNNR	$L^*$ , $*a$ , $*b$ , LAI	0.95	$3.75 \times 10^{-5}$
(Tilahun et al., 2018) [18]	LR	$*a$ , $*a/*b$	0.92, 0.94	
(Goisser et al., 2020) [28]	Exponential regression	$L^*$ , $a^*$ , $b^*$ , TCI	0.94, 0.90, 0.90, 0.91	

On the other hand, the electronic components' industrialization has lowered the products' costs such as cameras, touch screens, and minicomputers, and such is the case of the Raspberry Pi 4 where mathematical models were implemented. In addition, the RGB video camera and touch screen were connected to finally store all the method results in a micro USB flash drive. The advent of 3D printing also allowed us to build a functional and cheap prototype, and artificial intelligence gave us the opportunity to propose a lycopene estimation model with high reliability due to its low error with respect to HPLC. This same technology lets us use standard batteries in voltage and electrical current that allow the portability of the proposed sensor.

One of the main limitations of the investigation is the spectral range of operation, which is from 400 to 700 nm. Another limiting factor of the research is that the sensor must capture images of the samples under controlled lighting conditions. To develop a full picture of the measurement of Lycopene, we will need to increase the number of samples analyzed using HPLC. Further studies will need to be undertaken firmness, sugars, acidity, and tomato defects.

#### 4. Materials and Methods

##### 4.1. Samples

The characteristics and the number of samples were selected according to the methodology proposed by [16]. A total of 18 tomato samples that were produced in the Laja-Bajío region, Guanajuato, Mexico, were analyzed. These samples were selected with different degrees of maturity and homogeneous sizes. Tomatoes were visually classified into five maturity groups, as shown in Figure 4. These were composed of five green samples (G), three turned (T), three pink (P), two light red (LR), and five red (R). Figures 5 and 6 show the mapping of the samples using the RGB and lab color models. Consequently, it is observed that there is a relation between maturity and orthogonal axes.

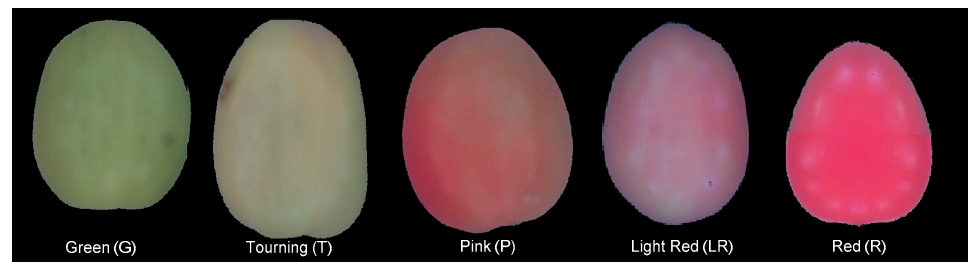


Figure 4. Tomato samples with different degrees of maturity.

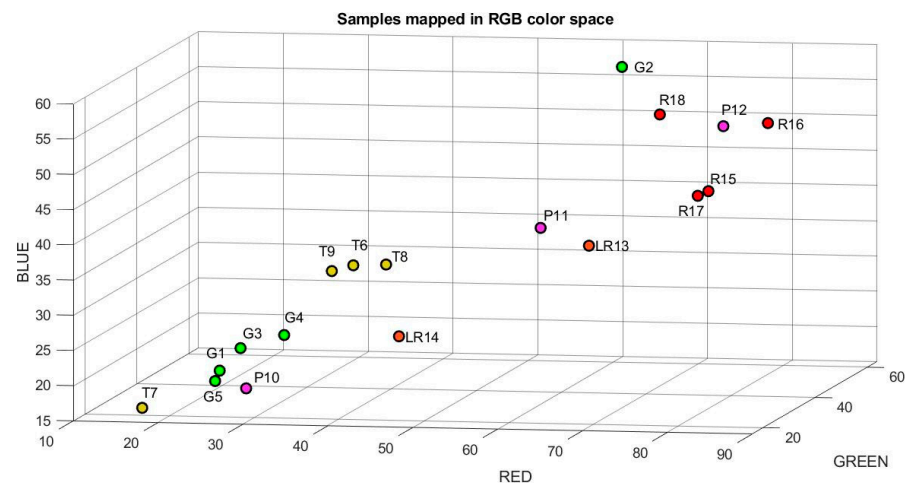
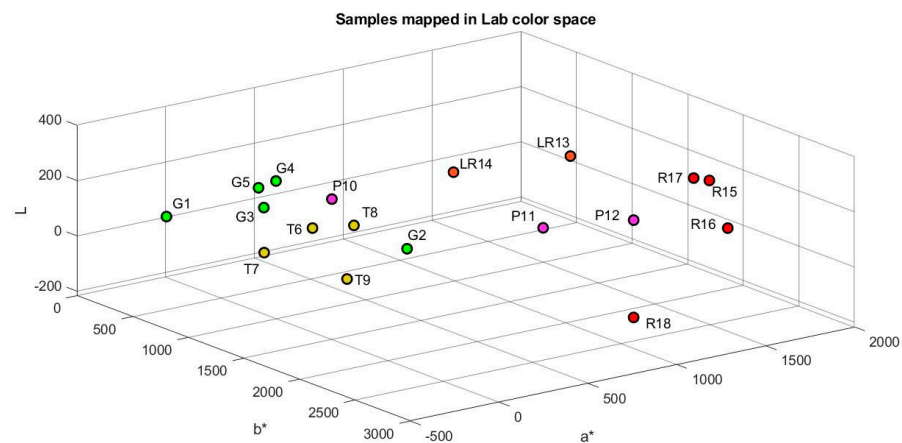


Figure 5. Mapping of the tomato samples using the RGB color space model.



**Figure 6.** Mapping of the tomato samples using the CIE-L\*a\*b\* color space model.

#### 4.2. HPLC Analysis

The extraction of lycopene from the tomatoes was based on the methodology proposed by [15,29]. The samples were washed with distilled water and dried carefully. The tomatoes were homogenized for 5 min with a sample blender. Carotenoid extraction was carried out using 5 g of each homogenized sample. Subsequently, they were added with a mixture of solvents (hexane/ethanol/acetone 50:25:25). It was immediately stirred for 5 min. Then, it was centrifuged for 5 min, and the supernatant was extracted. This was filtered through a membrane at 0.45  $\mu\text{m}$ . All solvents used were HPLC grade. Lycopene quantification was performed using an Agilent 1100 HPLC. This used a ZORBAX Eclipse XDB-C18 column (Agilent Technologies, Santa Clara, CA, USA) (4.6  $\times$  150 mm, 5  $\mu\text{m}$ ) that operated with an isocratic mobile phase with a flow rate of 1.2 mL/min of methanol and acetonitrile in a 4:6 ratio. The column temperature was 30  $^{\circ}\text{C}$ , and the absorbance was read at 475 nm. The calibration curve was obtained using a 95% pure lycopene standard (Sigma Chemical Co., St. Louis, MO, USA) and showed a retention time of 31 min. Figure 7 shows the chromatogram with the retention time (minutes). The retention peak area was 4457.5 mAU (milli-absorbance unit), corresponding to 89.285 ppm.

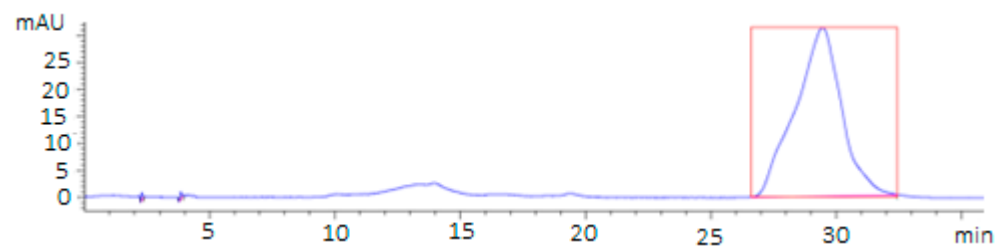


**Figure 7.** Lycopene measurement chromatogram.

#### 4.3. Sensor Developed

Figure 8a shows the sensor developed for measuring lycopene. This uses an 8 Megapixel Raspberry Pi 2 camera (Raspberry Pi Foundation, Cambridge, UK) that captures the reflection of light on the tomato. This light intensity is converted into a monochrome RGB image [29]. The processing of the RGB images was carried out by the Raspberry Pi 4 development board (Raspberry Pi Foundation) and an algorithm developed in OpenCV-Python 3. The sensor has a 17.78 cm or 7-inch touch screen that is an interface that shows the captured image and the lycopene content. This works with a 10,000 mAh 9 V/5 V 2 A power bank. Together, this has a semi-spherical semi-dome with a diameter of 10 cm that maintains diffuse illumination over the sample, as shown in Figure 8b [30]. It was built with an acrylonitrile butadiene styrene (ABS) filament that has good strength and low weight. In addition, this semi-dome has a camera and connector to place filters from the MIDOPT manufacturer. The lighting has a

ring-type architecture with eight white LEDs located at the same separation. This was selected for its ability to reduce the saturation of pixels in the capture of images by the camera. In addition, this sensor has an isolation system that is made up of a cylinder with a radius of 10 cm and a height that prevents disturbances from exterior lighting. This is the same material as the semi-spherical semi-dome. In addition, the architecture of the sensor can capture images using seven bandpass filters corresponding to the wavelengths of cyan, light green, orange, light red, dark red, and near-infrared/ultraviolet block-visible colors.

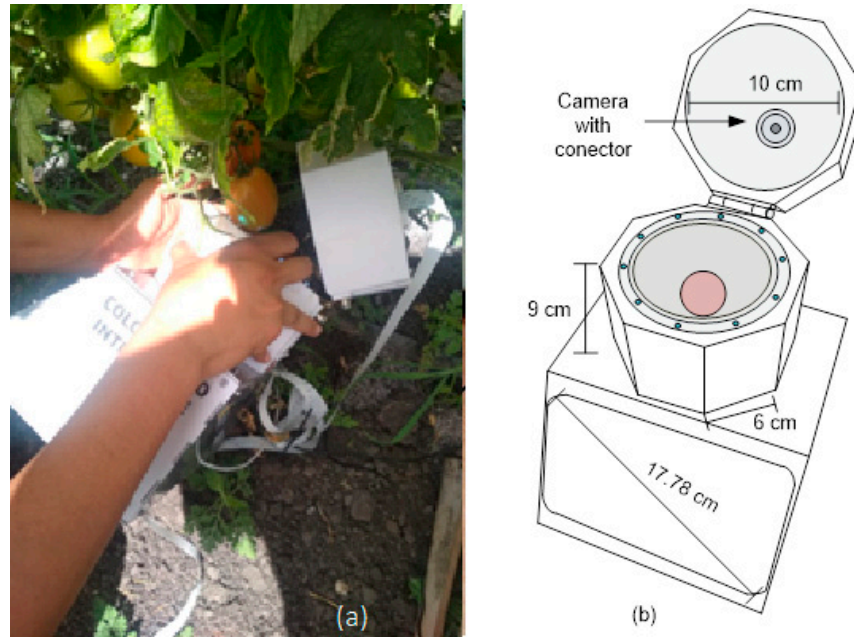


**Figure 8.** Proposed sensor for measuring lycopene in tomato: (a) Operation of the proposed sensor in the field, (b) Physical diagram of sensor.

#### 4.3.1. Sensor Device Configuration

Figure 9 shows the general scheme of the image processing algorithm proposed to predict lycopene content in tomato. This was integrated into four stages: the image acquisition, the image segmentation, obtaining the regions of interest to calculate areas, and prediction model evaluation.

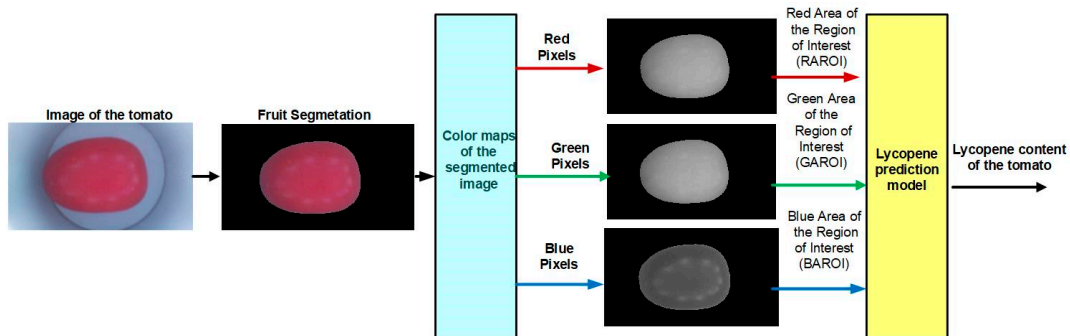


**Figure 9.** Scheme of the algorithm for the lycopene prediction in tomato.

#### 4.3.2. Image Acquisition

Seven RGB images were taken for each sample using seven filters, as shown in Figure 10. The image format was “JPG” with a resolution of  $768 \times 1366 \times 3$  [31]. The illumination spectrum is in the range of 400 to 800 nm [32]. This lighting affects the semi-dome in order to have diffuse lighting on the sample [33].

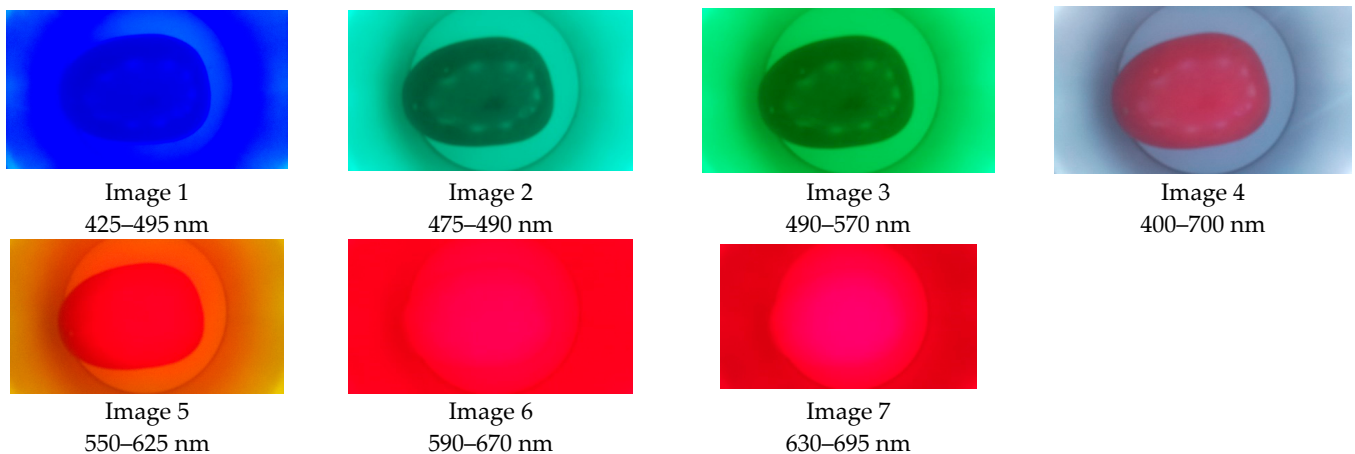


**Figure 10.** Images acquired by the sensor.

#### 4.3.3. Fruit Segmentation

The segmentation of the background of the sample was carried out using the HSV color space model. This has the advantage that the frequencies of each color in the visible spectrum can be identified. The H component is associated with the color hue, the purity of the color with the S component, and the proximity of the pixel to black and white with the V component. The segmentation was carried out with a range of H from 0.842 to 0.466, and for the case of S and V it was from 0 to 1. Figure 11 shows the results of the segmentation of the six views. Subsequently, the areas of pixels smaller than 400 that were not part of the samples were discriminated.

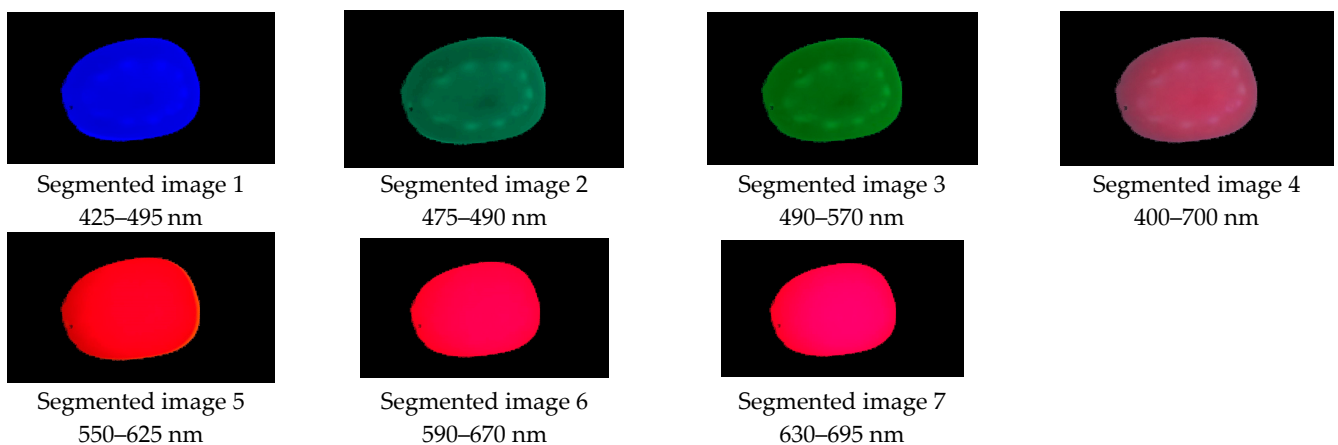


**Figure 11.** Images segmented by the sensor.

#### 4.4. Lycopene Estimator

##### 4.4.1. Artificial Neural Networks (ANNs)

Artificial neural networks (ANNs) are computational models that emulate the nervous system. These have become important due to their application in complex tasks of classification of maturity, shapes, and fruit defects. The ANNs are integrated by a set of neurons that are also known as nodes. The nodes can be classified as input, hidden, and output. The input nodes are stimulated by the information they receive from the outside. The hidden nodes are in charge of transmitting the information between the nodes of the network. The exit nodes send the processed information over the network [34,35].

Figure 12 shows the ANN architecture proposed to estimate the lycopene content. The proposed architecture has three layers. The first layer is the input, in which the training and validation data set corresponding to the color present in the tomato epicarp is presented. These correspond to the areas of the regions of interest corresponding to the red, green, and



blue pixels. The input layer used sigmoidal-type stimulated functions that are activated by the training pattern. The hidden layer adds the values of each neuron from the input layer that are multiplied. If the weight value is a positive number, it stimulates the next neuron. If the weight value is a negative number, then the next neuron will not be stimulated. The output layer is linear.

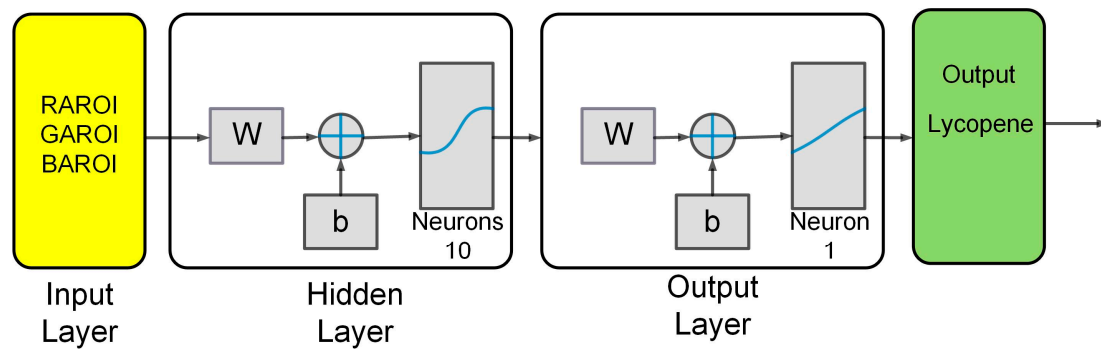


**Figure 12.** Artificial neuronal network predictor of lycopene.

Table 2 shows the characteristics of the proposed ANN models. The training of the models was carried out with the MATLAB Neuronal Network Toolbox. Model 1 used the regions of the RGB pixels, 10 neurons in the hidden layer of the sigmoidal type, and a linear output neuron as inputs. This achieved a correlation of  $R^2 = 0.98$  and an average error of 0.1684. The difference in Model 2 was the use of inputs in the  $L^*$ ,  $a^*$  and  $b^*$  pixel regions. This achieved a correlation of  $R^2 = 0.90$  and an average error of 0.5084. The proposed models are trained with the Levenberg–Marquardt algorithm. It has the advantages of a fast convergence mean square error (MSE) and an ability to approximate functions despite their complexity.

**Table 2.** Proposed models for measuring lycopene in tomatoes using ANNs.

Models	Technique	Entry	Neurons in the Hidden Layer Sigmoid	$R^2$	Error Mean	Epochs
Model 1	ANNs	R, G, B	10	0.9865	0.1684	10
Model 2	ANNs	$L^*$ , $a^*$ , $b^*$	10	0.9997	0.5084	10

#### 4.4.2. Fuzzy Logic (FL)

Fuzzy Logic (FL) is an artificial intelligence technique that allows you to analyze vague and imprecise data efficiently. This is based on the theory of fuzzy sets, which has the characteristics of utilizing an infinite number of truth values and linguist variables.

The main elements that integrate into a fuzzy system are fuzzification, inference, and defuzzification. Figure 13 shows the architecture of the fuzzy prediction system proposed for lycopene. The architecture has four inputs, one output, eight memberships, and eighteen rules of inference.

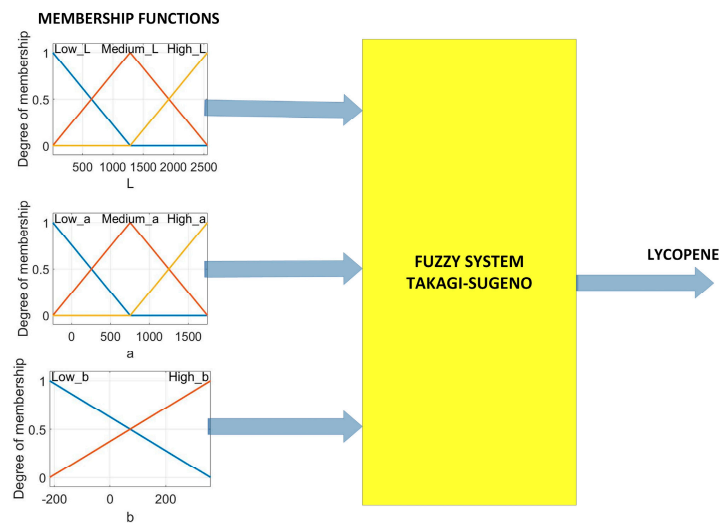


Figure 13. Fuzzy predictor of lycopene.

Fuzzification involves the transformation of real input variables into fuzzy values. This transformation aims to determine the degree of membership of the input. Triangular functions were applied to merge the variables, selecting them due to their easy implementation on the Raspberry Pi 3. The linguistic variables used were low, medium, and high. The mathematical equations corresponding to each membership function are detailed in Equations (1)–(8).

$$\text{Low}_L = \begin{cases} \frac{1285-L}{1285} & 0 < L \leq 1285 \\ 0 & 1285 < L \leq 2558.3 \end{cases} \quad (1)$$

$$\text{Medium}_L = \begin{cases} \frac{L-10.7}{1273} & 0 < L \leq 1285 \\ \frac{L-1285}{1273.7} & 1285 < L \leq 2558.3 \end{cases} \quad (2)$$

$$\text{High}_L = \begin{cases} 0 & 0 < L \leq 1285 \\ \frac{L-1273}{1273} & 1285 < L \leq 2558.3 \end{cases} \quad (3)$$

$$\text{Low}_a = \begin{cases} \frac{753-a}{753} & 0 < a \leq 753 \\ 0 & 753 < a \leq 1736 \end{cases} \quad (4)$$

$$\text{Medium}_a = \begin{cases} \frac{a}{753} & 0 < a \leq 753 \\ \frac{1736-a}{983} & 753 < a \leq 1736 \end{cases} \quad (5)$$

$$\text{High}_a = \begin{cases} 0 & 0 < a \leq 753 \\ \frac{a-753}{983} & 753 < a \leq 1736 \end{cases} \quad (6)$$

$$\text{Low}_b = \begin{cases} \frac{358-b}{148} & -210 < b \leq 358 \end{cases} \quad (7)$$

$$\text{High}_b = \begin{cases} \frac{b-210}{148} & -210 < b \leq 358 \end{cases} \quad (8)$$

Figure 14 represents the Takagi–Sugeno fuzzy model used for the development of the classifier. The reason for this choice was the ability of the ANFIS method to quickly train fuzzy systems with this architecture. Eighteen inference rules obtained from the fuzzy values of the regions of interest were used. The transformation of the classification output fuzzy values was performed using Equation (9). The final output is determined by rules using the  $Z_i$  output levels and the weight  $w_i$  of the rule. The method was chosen because it uses fuzzy rules and provides a series of linear functions as output. This model allows it to

analyze complex systems with larger dimensions than if the Mamdani method was used. All inference rules are found in Appendix A.

$$\text{Final output} = \frac{\sum_i^N w_i Z_i}{\sum_i^{18} w_i} \tag{9}$$

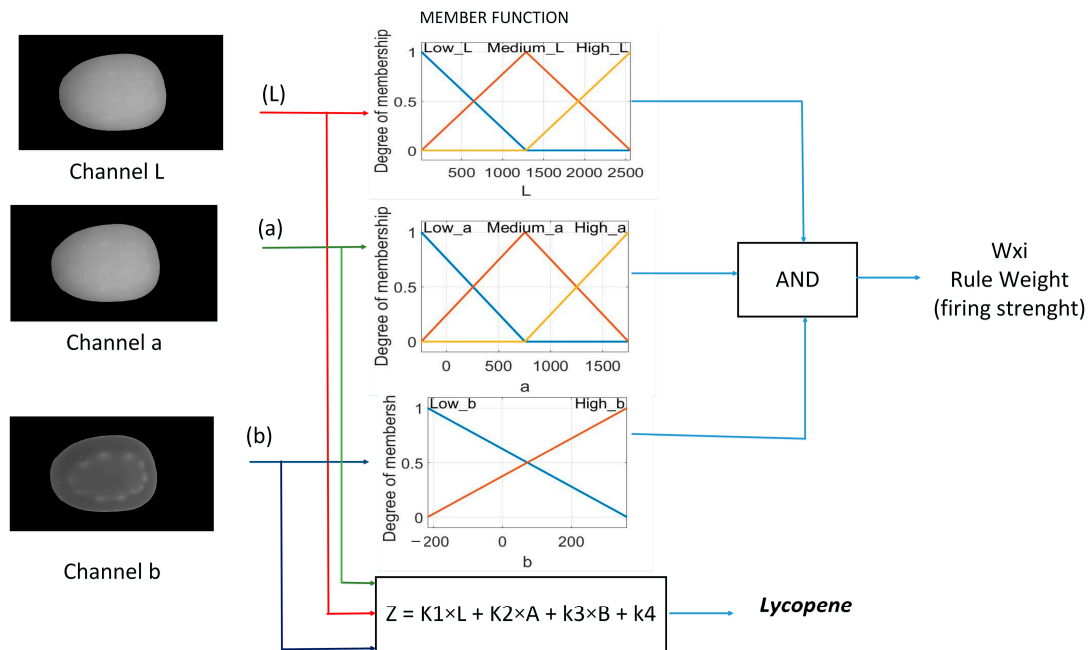


**Figure 14.** Operation of Takagi–Sugeno rules to estimate lycopene in tomato. The red line represents the luminance used in the fuzzification of the input. Also, it is used by the output level of the rule. The green and blue lines represent a and b chromaticity, respectively.

Table 3 shows the models that were evaluated in the sensor using FL. Model 1 was a linear regression (LR) using a\*/b\* transformed chromaticity. Models 2 and 3 were multiple nonlinear neuronal regressions (MNNR) using 10 neurons of the sigmoid type. Its inputs are the RGB and CIE-L\*a\*b color space components, respectively. For the case of Models 4 to 6, multiple nonlinear fuzzy regression (MNFR) was used. These models used two membership functions of the triangular type for each entry. The training of the models was carried out with the MATLAB Fuzzy Logic Designer.

**Table 3.** Proposed models for measuring lycopene in tomato using FL.

Models	Technique	Entry	Neurons in the Hidden Layer Sigmoid	Triangular Membership Features	R <sup>2</sup>	Error Mean	Epochs
Model 3	FL	R, G, B	-	8	0.9900	1.9 × 10 <sup>-5</sup>	10
Model 4	FL	L, *a, *b	-	8	0.9900	-0.9006	10
Model 5	FL	*a/*b	-	8	0.2896	-7.8 × 10 <sup>4</sup>	10
Model 6	FL	R, G	-	8	0.9900	-1.336 × 10 <sup>-6</sup>	10

### 5. Conclusions

In this work, a low-cost sensor for lycopene measurement in tomatoes was developed. High reliability was found according to the results obtained with Models 4, 5, and 6, which used fuzzy logic due to the low error with respect to the HPLC measurements. The results were also compared with recent works in the literature that validate our proposal. Qualitatively, it was observed that the proposed models are sensitive to lycopene

measurements at different stages of maturity. This supports the premise of measuring the lycopene content using the coloration present in the epicarp.

Regarding costs, the proposal is based on highly industrialized and standardized components, which helps to reduce the component's price. The cost of the sensor is around USD \$100–120. It offers the advantage of operating in a time reduced to seconds to estimate the lycopene content in tomatoes, which also reduces the cost of measurement. Moreover, the fact that it is a non-destructive measurement allows it to be a helpful sensor for the traceability of the tomato from the crop to the consumption. It should be highlighted that this sensor can be used to measure other variables regarding the quality of the fruits, such as firmness, sugars, acidity, and tomato damage. In particular, fruit carotenoids such as lutein, beta-carotene, beta-cryptoxanthin, and capsanthin can be estimated using the proposed method.

**Author Contributions:** M.-J.V.-A., J.-A.P.-M. and A.-I.B.-G.; methodology, J.-A.P.-M.; validation, J.-E.B.-Á.; formal analysis, M.-G.B.-S.; investigation, J.-A.P.-M.; writing—original draft preparation, J.P.-O. and M.-J.V.-A.; writing—review and editing, A.-I.B.-G.; supervision, A.-I.B.-G. All authors have read and agreed to the published version of the manuscript.

**Funding:** This research was funded by CONAHCyT, Sistema Nacional de Investigadores, IdeasGto, Tecnológico Nacional de México and Universidad Politécnica de Guanajuato.

**Data Availability Statement:** Data supporting reported results can be found at: [https://drive.google.com/drive/folders/1d1Q\\_RtEWmo2lbpipMCNG4x53s09-pB-C?usp=sharing](https://drive.google.com/drive/folders/1d1Q_RtEWmo2lbpipMCNG4x53s09-pB-C?usp=sharing).

**Conflicts of Interest:** The authors declare no conflict of interest.

## Appendix A

Listed below are the 18 inference rules and weights for each of the two fuzzy systems red, green, and blue:

1. If (L is Low\_L) and (a is Low\_a) and (b is Low\_b) then (Lycopene is Lycopemf1)
2. If (L is Low\_L) and (a is Low\_a) and (b is High\_b) then (Lycopene is Lycopemf2)
3. If (L is Low\_L) and (a is Medium\_a) and (b is Low\_b) then (Lycopene is Lycopemf3)
4. If (L is Low\_L) and (a is Medium\_a) and (b is High\_b) then (Lycopene is Lycopemf4)
5. If (L is Low\_L) and (a is High\_a) and (b is Low\_b) then (Lycopene is Lycopemf5)
6. If (L is Low\_L) and (a is High\_a) and (b is High\_b) then (Lycopene is Lycopemf6)
7. If (L is Medium\_L) and (a is Low\_a) and (b is Low\_b) then (Lycopene is Lycopemf7)
8. If (L is Medium\_L) and (a is Low\_a) and (b is High\_b) then (Lycopene is Lycopemf8)
9. If (L is Medium\_L) and (a is Medium\_a) and (b is Low\_b) then (Lycopene is Lycopemf9)
10. If (L is Medium\_L) and (a is Medium\_a) and (b is High\_b) then (Lycopene is Lycopemf10)
11. If (L is Medium\_L) and (a is High\_a) and (b is Low\_b) then (Lycopene is Lycopemf11)
12. If (L is Medium\_L) and (a is High\_a) and (b is High\_b) then (Lycopene is Lycopemf12)
13. If (L is High\_L) and (a is Low\_a) and (b is Low\_b) then (Lycopene is Lycopemf13)
14. If (L is High\_L) and (a is Low\_a) and (b is High\_b) then (Lycopene is Lycopemf14)
15. If (L is High\_L) and (a is Medium\_a) and (b is Low\_b) then (Lycopene is Lycopemf15)
16. If (L is High\_L) and (a is Medium\_a) and (b is High\_b) then (Lycopene is Lycopemf16)
17. If (L is High\_L) and (a is High\_a) and (b is Low\_b) then (Lycopene is Lycopemf17)
18. If (L is High\_L) and (a is High\_a) and (b is High\_b) then (Lycopene is Lycopemf18)

The coefficients obtained by the corresponding ANFIS are the following:

$$W1 = [-6.69138547328559 \quad -1.11067084181724 \quad 4.34025725184568 \quad 0.93184936978667]$$

$$W2 = [-0.318478847326583 \quad 5.64788126870901 \quad 3.59437092828302 \quad 0.58175498089429]$$

$$W3 = [3.95014047840935 \quad 1.59052198265991 \quad 3.3900952788002 \quad 0.299852425910745]$$

$$W4 = [19.5035468323403 \quad 6.38471348304066 \quad 4.78233606536508 \quad 0.202776907148019]$$

$$W5 = [0 \quad 0 \quad 0 \quad 0]$$

W6 = [0 0 0 0]  
 W7 = [3.16961759692625 2.58260252215251 -7.47834846471906 -0.0159918054557269]  
 W8 = [-2.49662488559166 -12.3987736560711 1.58390104162457 -0.0259522172477145]  
 W9 = [-0.963673706231771 -7.67628285198772 -14.882070217473 -0.000978530340102667]  
 W10 = [-1.17652671474686 4.28133259162214 8.58933040834423 -0.0180386146926471]  
 W11 = [27.6837746525357 30.0998637574663 -6.04580283260799 0.0125205680628005]  
 W12 = [-12.2501695143382 -9.11572464548948 1.28641408118073 -0.00567972816519314]  
 W13 = [3.89196417128968 -5.62446094757007 0.449363113520893 0.00425330019057446]  
 W14 = [2.09041280770293 -14.8185805057198 1.75403548818368 0.0086653984730775]  
 W15 = [-3.74341236002276 -16.3575329602085 -13.1859975500766 -0.0010654550733953]  
 W16 = [25.7278702631458 -27.0060723666553 22.5846060837755 0.0254252141584876]  
 W17 = [-17.3655978345049 16.2129055618654 -5.54378482385434 -0.00225230673875521]  
 W18 = [-24.9130829636862 38.4699087639502 1.82213892573319 -0.0116749561770817]

## References

1. Tilesi, F.; Lombardi, A.; Mazzucato, A. Scientometric and Methodological Analysis of the Recent Literature on the Health-Related Effects of Tomato and Tomato Products. *Foods* **2021**, *10*, 1905. [CrossRef]
2. FAOSTAT 2023. Available online: <http://www.fao.org/faostat/> (accessed on 28 March 2023).
3. Ali, M.Y.; Sina, A.A.I.; Khandker, S.S.; Neesa, L.; Tanvir, E.M.; Kabir, A.; Khalil, M.I.; Gan, S.H. Nutritional Composition and Bioactive Compounds in Tomatoes and Their Impact on Human Health and Disease: A Review. *Foods* **2021**, *10*, 45. [CrossRef]
4. Ye, X.; Izawa, T.; Zhang, S. Rapid determination of lycopene content and fruit grading in tomatoes using a smart device camera. *Cogent. Eng.* **2018**, *5*, 1504499. [CrossRef]
5. Gryech, I.; Ben-Aboud, Y.; Guermah, B.; Sbihi, N.; Ghogho, M.; Kobbane, A. MoreAir: A Low-Cost Urban Air Pollution Monitoring System. *Sensors* **2020**, *20*, 998. [CrossRef] [PubMed]
6. Meng, C.; Yang, D.; Ma, X.; Zhao, W.; Liang, X.; Ma, N.; Meng, Q. Suppression of tomato SINAC1 transcription factor delays fruit ripening. *J. Plant Physiol.* **2016**, *193*, 88–96. [CrossRef] [PubMed]
7. Rosati, C.; Aquilani, R.; Dharmapuri, S.; Pallara, P.; Marusic, C.; Tavazza, R.; Giuliano, G. Metabolic engineering of beta-carotene and lycopene content in tomato fruit. *Plant J.* **2000**, *24*, 413–420. [CrossRef] [PubMed]
8. Mignani, A.G.; Ciaccheri, L.; Mencaglia, A.A.; Tuccio, L.; Agati, G. Application of a LED-based reflectance sensor for the assessing in situ the lycopene content of tomatoes (*Lycopersicon esculentum* Mill.). In Proceedings of the Sensing for Agriculture and Food Quality and Safety VII, Baltimore, MD, USA, 20–24 April 2015. [CrossRef]
9. Hussain, A.; Pu, H.; Sun, D. Measurements of lycopene contents in fruit: A review of recent developments in conventional and novel techniques. *Crit. Rev. Food Sci. Nutr.* **2018**, *59*, 758–769. [CrossRef] [PubMed]
10. Villaseñor-Aguilar, M.-J.; Padilla-Medina, J.-A.; Botello-Álvarez, J.-E.; Bravo-Sánchez, M.-G.; Prado-Olivares, J.; Espinosa-Calderon, A.; Barranco-Gutiérrez, A.-I. Current Status of Optical Systems for Measuring Lycopene Content in Fruits: Review. *Appl. Sci.* **2021**, *11*, 9332. [CrossRef]
11. Kulkarni, A.S.; Ghugre, P.S.; Udipi, S.A. Applications of nanotechnology in nutrition: Potential and safety issues. In *Novel Approaches of Nanotechnology in Food*, 1st ed.; Grumezescu, A.M., Ed.; Academic Press: Cambridge, MA, USA, 2016; Volume 1, pp. 509–554.
12. Skoog, D.A.; Holler, F.J.; Crouch, S.R. Separation Methods. In *Principles of Instrumental Analysis*, 7th ed.; Cengage Learning: Boston, MA, USA, 2018; pp. 746–781.
13. Van den Berg, H.; Faulks, R.; Granado, H.F.; Hirschberg, J.; Olmedilla, B.; Sandmann, G.; Stahl, W. The potential for the improvement of carotenoid levels in foods and the likely systemic effects. *J. Sci. Food Agric.* **2000**, *80*, 880–912. [CrossRef]
14. Parrini, S.; Acciaioli, A.; Franci, O.; Pugliese, C.; Bozzi, R. Near infrared spectroscopy technology for prediction of chemical composition of natural fresh pastures. *J. Appl. Anim. Res.* **2019**, *47*, 514–520. [CrossRef]
15. Arias, R.; Lee, T.-C.; Logendra, L.; Janes, H. Correlation of lycopene measured by HPLC with the L\*, a\*, b\* color readings of a hydroponic tomato and the relationship of maturity with color and lycopene content. *J. Agric. Food Chem.* **2000**, *48*, 1697–1702. [CrossRef] [PubMed]
16. Begum, N.; Hazarika, M.K. Maturity detection of tomatoes using transfer learning. *Meas. Food* **2022**, *7*, 100038. [CrossRef]
17. Vazquez-Cruz, M.A.; Jimenez-Garcia, S.N.; Luna-Rubio, R.; Contreras-Medina, L.M.; Vazquez-Barrios, E.; Mercado-Silva, E.; Torres-Pacheco, I.; Guevara-Gonzalez, R.G. Application of neural networks to estimate carotenoid content during ripening in tomato fruits (*Solanum lycopersicum*). *Sci. Hort.* **2013**, *162*, 165–171. [CrossRef]
18. Tilahun, S.; Park, D.S.; Seo, M.H.; Hwang, I.G.; Kim, S.H.; Choi, H.R.; Jeong, C.S. Prediction of lycopene and  $\beta$ -carotene in tomatoes by portable chroma-meter and VIS/NIR spectra. *Postharvest Biol. Technol.* **2018**, *136*, 50–56. [CrossRef]
19. Ropelewska, E.; Szwejda-Grzybowska, J. Relationship of Textures from Tomato Fruit Images Acquired Using a Digital Camera and Lycopene Content Determined by High-Performance Liquid Chromatography. *Agriculture* **2022**, *12*, 1495. [CrossRef]

20. Kondaveeti, H.K.; Bandi, D.; Mathe, S.E.; Vappangi, S.; Subramanian, M. A review of image processing applications based on Raspberry-Pi. In Proceedings of the 2022 8th International Conference on Advanced Computing and Communication Systems (ICACCS), Coimbatore, India, 25–26 March 2022; Volume 1, pp. 22–28.
21. Li, J.; Huang, W.; Zhao, C. Machine vision technology for detecting the external defects of fruits | A review. *Imaging Sci.* **2015**, *63*, 241–251. [[CrossRef](#)]
22. Timmermans, A.J.M. Computer vision system for on-line sorting of pot plants based on learning techniques. In Proceedings of the II International Symposium on Sensors in Horticulture 421, Greve, Denmark, 21 August 1995; pp. 91–98. [[CrossRef](#)]
23. Rajkumar, P.; Wang, N.; Elmasry, G.; Raghavan, G.; Garipey, Y. Studies on banana fruit quality and maturity stages using hyperspectral imaging. *J. Food Eng.* **2012**, *188*, 194–200. [[CrossRef](#)]
24. Santoyo-Mora, M.; Sancen-Plaza, A.; Espinosa-Calderon, A.; Barranco-Gutierrez, A.I.; Prado-Olivarez, J. Nondestructive quantification of the ripening process in banana (musa aab simmonds) using multispectral imaging. *J. Sens.* **2019**, *2019*, 6742896. [[CrossRef](#)]
25. Shetty, D.K.; Acharya, U.D.; Malarout, N.; Gopakumar, R.; Prajwal, P.J. A review of application of computer-vision for quality grading of food products. In Proceedings of the 2019 International Conference on Automation, Computational and Technology Management (ICACTM) IEEE, London, UK, 24–26 April 2019. [[CrossRef](#)]
26. Villaseñor-Aguilar, M.-J.; Botello-Álvarez, J.E.; Pérez-Pinal, F.J.; Cano-Lara, M.; León-Galván, M.F.; Bravo-Sánchez, M.-G. Fuzzy-Classification of the maturity of the tomato using a vision system. *J. Sens.* **2019**, *2019*, 3175848. [[CrossRef](#)]
27. Barba, A.I.O.; Hurtado, M.C.; Mata, M.C.S.; Ruiz, V.F.; Tejada, M.L.S. De Application of a UV-vis detection-HPLC method for a rapid determination of lycopene and  $\beta$ -carotene in vegetables. *Food. Chem.* **2006**, *95*, 328–336. [[CrossRef](#)]
28. Goisser, S.; Wittmann, S.; Fernandes, M.; Mempel, H.; Ulrichs, C. Comparison of colorimeter and different portable food-scanners for non-destructive prediction of lycopene content in tomato fruit. *Postharvest Biol. Technol.* **2020**, *167*, 111232. [[CrossRef](#)]
29. Wu, D.; Sun, D.-W. Colour measurements by computer vision for food quality control—A review. *Trends Food Sci. Technol.* **2013**, *29*, 5–20. [[CrossRef](#)]
30. Lorente, D.; Blasco, J.; Serrano, A.J.; Soria-Olivas, E.; Aleixos, N.; Gómez-Sanchís, J. Comparison of ROC feature selection method for the detection of decay in citrus fruit using hyperspectral images. *Food Bioprocess Technol.* **2013**, *6*, 3613–3619. [[CrossRef](#)]
31. Pagnutti, M.; Ryan, R.E.; Cazenavette, G.; Gold, M.; Harlan, R.; Leggett, E.; Pagnutti, J. Laying the foundation to use Raspberry Pi 3 V2 camera module imagery for scientific and engineering purposes. *J. Electron. Imaging* **2017**, *26*, 013014. [[CrossRef](#)]
32. Azarndel, H.; Jahanbakhshi, A.; Mohtasebi, S.S.; Muñoz, A.R. Evaluation of image processing technique as an expert system in mulberry fruit grading based on ripeness level using artificial neural networks (ANNs) and support vector machine (SVM). *Postharvest Biol. Technol.* **2020**, *166*, 111201. [[CrossRef](#)]
33. Wan, P.; Toudeshki, A.; Tan, H.; Ehsani, R. A methodology for fresh tomato maturity detection using computer vision. *Comput. Electron. Agric.* **2018**, *146*, 43–50. [[CrossRef](#)]
34. Kokka, A.; Poikonen, T.; Blattner, P.; Jost, S.; Ferrero, A.; Pulli, T.; Ngo, M.; Thorseth, A.; Gerloff, T.; Dekker, P.; et al. Development of white LED illuminants for colorimetry and recommendation of white LED reference spectrum for photometry. *Metrologia* **2018**, *55*, 526–534. [[CrossRef](#)]
35. Fashi, M.; Naderloo, L.; Javadikia, H. The relationship between the appearance of pomegranate fruit and color and size of arils based on image processing. *Postharvest Biol. Technol.* **2019**, *154*, 52–57. [[CrossRef](#)]

**Disclaimer/Publisher’s Note:** The statements, opinions and data contained in all publications are solely those of the individual author(s) and contributor(s) and not of MDPI and/or the editor(s). MDPI and/or the editor(s) disclaim responsibility for any injury to people or property resulting from any ideas, methods, instructions or products referred to in the content.